BEAM-BEAM EFFECTS IN ELECTRON AND PROTON COLLIDERS

Eberhard Keil
CERN
CH-1211 Geneva 23, Switzerland

Summary

This review of beam-beam effects in electron and proton colliders is divided into two main parts, the first devoted to electron-positron colliders and the second to proton-antiproton colliders. Both parts start with a discussion of recent observations in existing colliders. The part on electron-positron colliders continues with a discussion of the frequencies of the coherent oscillations of the rigid bunches coupled by the beam-beam forces, and concludes with a discussion of several attempt to understand the nature of the beam-beam interaction theoretically. The part on proton-antiproton colliders continues with an interpretation of the observations in terms of the tune spreads present in the colliding beams, and concludes with a discussion of the observed distribution functions.

1. Introduction

This review of beam-beam effects in electron and proton colliders consists of two main parts. Chapter 2 contains the discussion of beam-beam effects in electron-positron colliders, and Chapter 3 the discussion of proton-antiproton colliders. Both chapters have their own introductions and conclusions. Chapter 4 contains final remarks.

2. Beam-beam Effect in Electron-Positron Colliders

In this chapter, recent studies of the beam-beam effect in electron-positron colliders are presented. It is organized as follows: In Sect. 2.1 recent observations of the beam-beam tune shift are summarized, in Sect. 2.2 the coherent beam-beam effect is described, and in Sect. 2.3 theoretical studies of the nature of the beam-beam limit are discussed.

The luminosity L and the beam-beam strength parameter ξ_y for vertical betatron oscillations play a central role in the discussion of electron-positron colliders. They are given by:

$$L = \frac{N^2 fk}{4\pi \sigma_x \sigma_y} \tag{1}$$

$$\xi_y = \frac{r_e}{2\pi} \frac{N \beta_y}{\gamma \sigma_y(\sigma_x+\sigma_y)} \tag{2}$$

Here, the symbols are defined as follows: r_e is the classical electron radius, N is the number of particles in a bunch, γ is the relativistic factor, β_y is the vertical amplitude function, σ_x and σ_y are the horizontal and vertical rms beam radii, respectively, at the crossing point, f is the revolution frequency in the collider, and k is the number of bunches in one beam (fk is the bunch collision frequency). Both equations are derived under the assumption that the variation of β_y, σ_x and σ_y along the beam direction can be neglected in the neighbourhood of the collision point. This assumption is well satisfied if the bunch-length σ_s is small compared to β_x and β_y. If this assumption does not hold, the strength parameter ξ_y increases [1], and the luminosity L decreases [2]. The beam-beam strength parameter for horizontal betatron oscillations ξ_x is obtained from Eq. (2) by replacing β_y and σ_y by β_x ands σ_x, respectively. For $\xi_y \to 0$, Eq. (2) describes the vertical tune shift for test particles with betatron oscillation amplitudes small compared to σ_x and σ_y, and is therefore often loosely called the beam-beam tune shift.

Eq. (2) may be used to eliminate one power of N from Eq. (1), casting it into a form which shows both limitations on the performance of electron-positron storage rings, (i) the bunch current I and (ii) the beam-beam strength parameter ξ_y, in the approximation $\sigma_y \ll \sigma_x$, and with the electron charge e:

$$L = \frac{I\gamma \xi_y k}{2er_e\beta_y} \tag{3}$$

An absolute measurement of the quantities entering into Eq. (3) is one way of determining ξ_y. In Eq. (3) it is assumed that it is possible to adjust the beam radii σ_x and σ_y such that the beam-beam strength limit ξ_y is just reached at the bunch current I.

2.1 Recent observations in electron-positron colliders

Two new electron-positron colliders have recently come into operation, TRISTAN at the KEK Laboratory in Tsukuba, Japan [3], and BEPC at the Institute of High Energy Physics in Beijing, China [4]. Their relevant parameters and observations of the beam-beam strength parameters are summarized in Table 1. It should be noted that the current quoted in [3] is the total current in both beams.

	BEPC	Tristan
Energy E/GeV	1.6	26
Bunch current I/mA	16	2.2
Circumference C/m	240.4	3018
Vertical damping time τ_y/ms	46	3.2
Amplitude fct. β_y/m	0.085	0.1
Bunches/beam k	1	2
Luminosity $L/10^{30}cm^{-2}s^{-1}$	2	7.2
Beam-beam strength ξ_y	0.031	0.032

Table 1 - Parameters of electron colliders

Comparing these data to a compilation [5] of beam-beam strength limits ξ_y shows that the observations in the new machines fall into the range of the observations in earlier machines. This confirms the opinion that the beam-beam strength parameter a good variable for describing the beam-beam effect because it shows relatively little variation over machines in a wide range of energy and size.

2.2 Coherent beam-beam effect

The coherent beam-beam effect describes the motion of the centres of gravity of rigid electron and positron bunches in a storage ring. In the usual approximation, the bunches perform linear oscillations between the collision points, and are coupled by the beam-beam forces at the collision points. Much confusion has arisen because different authors have made different assumptions about the ratio between the number k of bunches in one beam, assumed to be equal to the number of bunches in the other beam, and the number of collision points n_x: some authors take $n_x = k$, and others take $n_x = 2k$ which corresponds to practical operating configurations. In this paper, I shall use $n_x = 2k$, as in my earlier writings.

2.2.1 Linear theory. If the beam-beam force is linearized, the stability of the bunch motion can be investigated separately in the horizontal and vertical plane, and be reduced to a computation of the eigenvalues of matrices of order 4k which are products of 2k

CH2669-0/89/0000-1731$01.00©1989 IEEE

(2×2) block-diagonal matrices describing the bunch motion in the arcs, alternating with 2k kick matrices describing the bunch collisions. In the simplest case, with k = 1, one finds two modes. The σ-mode has the frequency Q of the betatron oscillations in the absence of the beam-beam collisions; the π-mode has a higher (lower) frequency for particle-antiparticle (particle-particle) collisions, approximately given by:

$$Q_\pi \simeq Q_\sigma \pm n_x \, \delta Q_y \tag{4}$$

Here δQ_y is the coherent beam-beam tune shift due to a single beam-beam collision. For k > 1, there are 2k modes, but there remains a mode with the unperturbed frequency Q, and a mode with the largest frequency shift which is still given by Eq. (4).

Piwinski [6] and Chao and Keil [7] obtained the beam-beam kicks $\delta'_{y\pm}$ from the beam-beam strength parameter ξ_y:

$$\delta'_{y\pm} = \pm \frac{4\pi\xi_y(y_+ - y_-)}{\beta_y} \tag{5}$$

Here the indices - and + label the electron and positron beam. This leads to a coherent beam-beam strength parameter δQ_y which was exactly twice the incoherent one $\delta Q_y = 2\xi_y$. Hence, the tune difference between the π- and σ-modes for k = 1 becomes approximately $4\xi_y$. This rule of thumb is only an approximation, valid for $\xi_y \to 0$, [6] gives the exact expression.

The frequency difference between the π and σ modes was also observed in electron-positron colliders [8] and obtained by Fourier analyzing the motion of the bunch centres in a multi-particle beam-beam simulation [9, 10]. An example of such a simulation is shown in Fig. 1. In both cases it was found that the frequency difference $Q_\pi - Q_\sigma$ was about 2/3 of that expected from Eq. (4).

This discrepancy can be understood. The incoherent beam-beam tune shift is due to the kick which a test particle receives when it travels through the bunch at a distance $y \ll \sigma_y$. What matters for the coherent beam-beam tune shift δQ_y is the kick which a whole test bunch receives when it travels through the bunch at a distance $y \ll \sigma_y$, obtained by integrating the kick over the whole test bunch with a weight corresponding to the density distribution in it. Talman [8], Hirata [11] and Hofmann and Myers [12] have done this integration and obtained a coherent beam-beam strength parameter δQ_y which is a factor of two smaller, $\delta Q_y = \xi_y$, for $y_+ - y_- \ll \sigma_y$, leading to the result, in the limit $\xi_y \to 0$:

$$Q_\pi - Q_\sigma \simeq n_x \xi_y \tag{6}$$

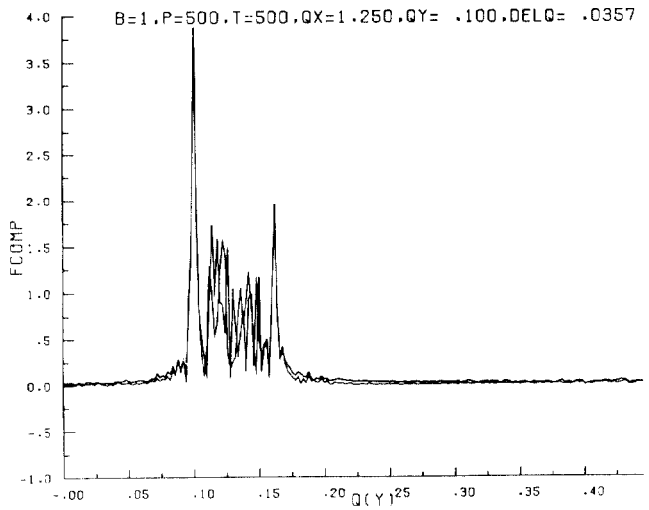

Fig.1 - Frequency spectrum of coherent vertical beam-beam oscillations for k = 1, n_x = 2, Q_x = 1.25, ξ_y = 0.0357.

2.2.2 Nonlinear theory. In nonlinear theory, the forces due to the beam-beam collisions are used to construct the Vlasov equation of the particle distribution in action-angle variables. Averaging over the angles, an integral equation is obtained, in which the ratio of the coherent and incoherent beam-beam strength parameters appears as an eigenvalue $\lambda_y = \delta Q_y/\xi_y$. Expanding into orthogonal polynomials, the equation for λ_y becomes a matrix eigenvalue problem after truncation to finite order. Meller and Siemann [13] used Legendre polynomials and found $\lambda_y = 1.34$. Yokoya [14] used Laguerre polynomials and obtained the values of $\lambda_x = \delta Q_x/\xi_x$ and $\lambda_y = \delta Q_y/\xi_y$ as functions of the axis ratio parameter $r = \sigma_y/(\sigma_x+\sigma_y)$. His results can be fitted to better than a percent by the following expression:

$$\lambda_x(r) = 1.330 - 0.370r + 0.279r^2 \tag{7}$$

while

$$\lambda_y(r) = \lambda_x(1-r) \tag{8}$$

An amusing by-product of this calculation is shown in Fig. 2, a coherent horizontal oscillation with the eigenvalue λ_x and an amplitude of 0.1 σ_x. It may be seen that the mode does not involve a shift of the Gaussian density distribution as a whole. Instead, the core of the beam oscillates and the tails remain practically stationary.

2.3 Beam-beam limit

In the early 1980's, several multi-particle simulations of the beam-beam effect [15, 16, 17, 18] had obtained satisfactory agreement with experimental data. They all used the strong-strong model in which the beam-beam forces act on both beams and modify their motion. This is in contrast to the weak-strong model where the particles of the weak test beam are subject to the forces of the strong beam which itself is not affected by the forces of the test beam. More recently, there has been less activity in beam-beam simulation. Instead, there have been several attempts to obtain the beam-beam limit by analytical methods, which I shall discuss now.

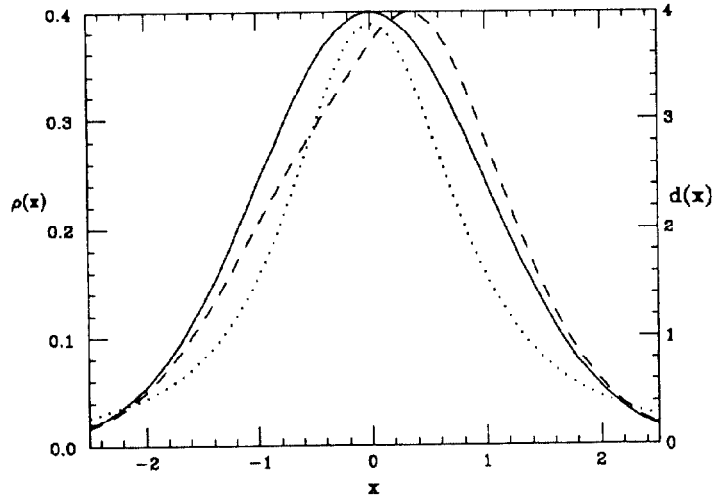

Fig.2 - Coherent horizontal bunch oscillation. Solid line: equilibrium Gaussian, dashed line: coherent oscillation with c.m. shift 0.1σ_x.

2.3.1 Maps of the second moments of distribution functions. An ideal solution to the dynamics of two colliding beams must be self-consistent, i.e. the phase-space distribution functions of both beams must satisfy the Vlasov equation at all times, and the forces seen by any particle must be obtained from the distribution function by the Maxwell equation. This formidable problem has been looked at in various approximations.

Hirata [19] and Furman, Ng and Chao [20] have studied the one-turn maps for the second moments of the distribution functions in colliding beams. The ingredients of their calculations are:

(i) Beam-beam kicks which are functions of the size of the opposite bunch. Hirata calculates the forces for a Gaussian density distribution. Furman, Ng and Chao assume that the force is linear.

(ii) Radiation damping, described by the decrement $\delta \ll 1$ between collisions.

(iii) Quantum excitation which compensates the radiation damping such that an equilibrium is reached - in the absence of beam-beam forces - at the unperturbed beam dimensions.

(iv) Linear transformations with phase advance $2\pi\nu$ between the kicks. In both papers, one beam-beam collision is assumed in a revolution.

In either case, a map is obtained which describes the transformation of the canonical scaled variables ($q_\pm$, $p_\pm$) through one revolution. It is transformed into another map which describes the transformation of the lowest moments $\langle q_\pm^2 \rangle$, $\langle q_\pm p_\pm \rangle$ and $\langle p_\pm^2 \rangle$ through one revolution. This map is non-trivial because it not only operates on the moments, but also contains them in the coefficients.

Since Hirata applies a nonlinear force derived from a Gaussian distribution in phase space, he introduces an inconsistency with the Vlasov equation into his calculation because a Gaussian distribution in phase space cannot remain Gaussian under the influence of a nonlinear force. Furman, Ng and Chao avoid this difficulty by assuming a linear force, thus ignoring the Maxwell equations altogether. Their approximation only holds for particles with amplitudes small compared to the rms beam radii. It overestimates the force on all particles, and by a large factor that on particles in the tail of the distribution function at several rms beam radii.

Hirata finds the map for the moments in the case of round beams, Furman, Ng and Chao find it both for round and flat beams. They then proceed to obtain the fixed points with period one, i.e. stationary solutions for the moments which repeat on every revolution. Furman, Ng and Chao also linearize the map in the neighbourhood of the fixed point and analyze its stability. Both authors iterate the map for many revolutions and compare the results to those of their analytical results. The map depends on the following parameters:

(i) The phase advance $2\pi\nu$ between collision points, or the tune ν.

(ii) The damping decrement δ between collision points, or the parameter $\lambda = \exp(-2\delta)$.

(iii) The unperturbed beam-beam strength parameter ξ_0, calculated in the absence of changes to the rms beam radii.

(iv) The beam shape, flat or round.

An example of results is shown in Fig.3 taken from [20]. It gives the rms beam-size for a flat beam as a function of ξ_0. The abscissa is $\rho = 4\pi\xi_0/(1+\lambda) \approx 6.722\ \xi_0$. For $0 < \rho < 0.4$, both beams have the same size which shrinks with increasing ρ, presumably due to the dynamic β effect which reduces β at the collision point while ξ_0 increases for the tune of the example. Between $0.4 < \rho < 1.4$, i.e. $0.06 < \xi_0 < 0.21$, the map is unstable. Iteration of the map just above $\xi_0 = 0.06$ shows chaotic behaviour, i.e. the beam radii vary from turn to turn with no apparent regularity. At $\rho = 1.4$, $\xi_0 = 0.21$, a bifurcation occurs, and the sizes of the two beams become vastly different, one is blown up, the other one shrinks. The beam size is stable between $1.5 < \rho < 2.0$. Hirata [20] observes a similar bifurcation, and relates it to the flip-flop effect, where one beam is indeed blown up and the other one shrinks, which has been observed in SPEAR [21] and in computer simulations [18]. In SPEAR, the effect was observed for $\xi_0 > 0.025$. In simulations, the flip-flop effect has been observed for $\xi_0 = 0.06$, i.e. a factor of 3.5 smaller than in Fig. 3.

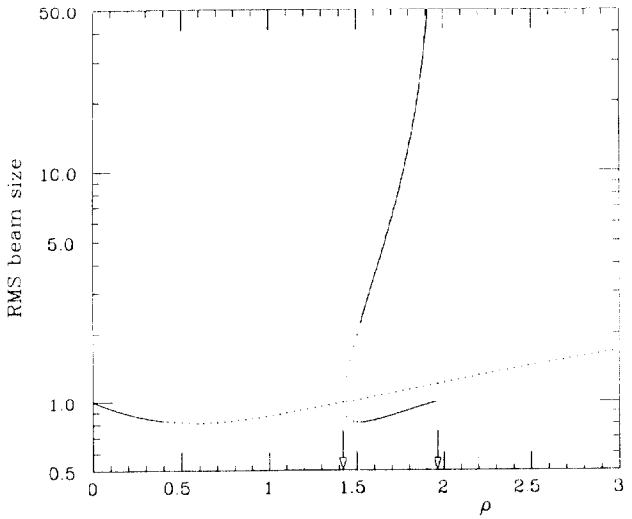

Fig.3 - RMS beam sizes and stability for the period-1 fixed point solutions (solid = stable, dots = unstable). Flat-beam case, $\nu = 0.15$, $\lambda = 0.8694$.

By iterating the map, Furman, Ng and Chao also find fixed points with period two, three and four which Hirata does not find. This is believed to be due to the different assumptions about the beam-beam force.

Hirata [22] has developed a technique to include higher than the second moments. The results are not very different from his earlier results [19].

2.3.2 Renormalized theory. A renormalized theory of the beam-beam interaction in electron-positron colliders was developed and implemented by Chin [23, 24], who calculated an approximate solution to the Fokker-Planck equation for the stationary particle distribution function. The formalism avoids the secular terms of conventional perturbation theory which cause it to diverge in the neighbourhood of resonances if the perturbation series is truncated after a few terms.

The formalism is derived in the approximation of one-dimensional motion, i.e. a round beam, and of collisions between a weak test beam with a strong beam with Gaussian density distribution. The result is the distribution function $P(I)$ in terms of the action I for the weak beam. In principle, the knowledge of the distribution function, including its tails, allows to calculate the beam lifetime in the presence of the beam-beam effect, and therefore to establish a relation between the observation in existing machines that the lifetime suddenly drops when the beam-beam strength parameter ξ exceeds a given value.

The formalism is implemented in a computer program. An associated tracking program allows a comparison between theory and simulation. Fig. 4 shows an example of the results in a region of tune space with only high-order resonances and a rather high value of ξ. The density distribution is more exponential than Gaussian and the agreement between theory and simulation is very good. Another characteristic feature of this theory is pedestals in the distribution function when strong low-order resonances occur at a few rms beam radii.

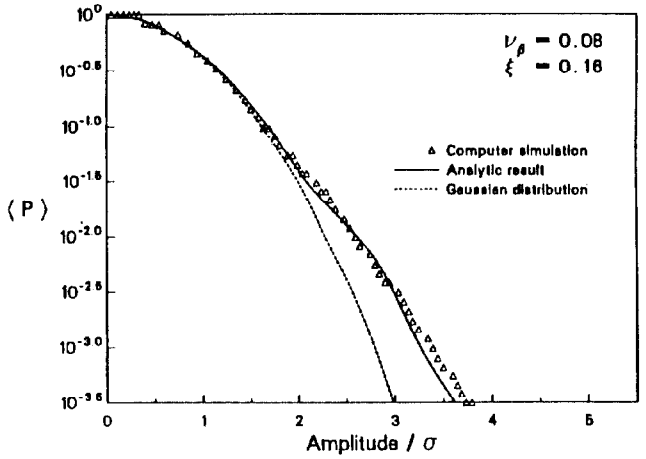

Fig.4 - Particle distributions for ν=0.08 and ξ=0.16.

2.4 Conclusions for electron colliders

Two new machines, TRISTAN and BEPC, came into operation recently. From the point of view of beam-beam effects, they show no surprises. The coherent dipole beam-beam effect has been worked on for nearly twenty years. There now is a consensus how it should be calculated, and agreement between theory and observation. Several interesting attempts to explain the beam-beam have been published. The authors needed drastic simplifications, i.e. one rather than two dimensions, simple forces, lack of self-consistency, weak-strong model, to deal with the mathematics. This makes it difficult to compare theory with observations in existing colliders to check their validity, and to exploit their predictive power. However, the removal of all simplifications is a formidable problem which might not ever be solved.

3. Beam-Beam Effects in Proton Colliders

In this chapter, recent studies of the beam-beam in proton-antiproton colliders are presented. It is organized as follows: In Sect. 3.1 recent observations are summarized which are discussed in Sect. 3.2 in terms of the tune spreads and density distribution of the beams.

In contrast to electron-positron colliders where the colliding beams are flat, the colliding beams in proton colliders are usually very nearly round. Assuming that this holds exactly, i.e. that the rms beam radii are equal, $\sigma_x = \sigma_y = \sigma$, and that the amplitude functions at the collision points are also equal, $\beta_x = \beta_y = \beta$, the equations for luminosity L and the beam-beam strength parameter ξ may be written as follows, assuming also that the proton and antiproton beams are equal:

$$L = \frac{N^2 f k}{2\pi\sigma^2} \qquad (9)$$

$$\xi = \frac{N r_p \beta_y}{4\pi\gamma\sigma^2} = \frac{N r_p}{\varepsilon} \qquad (10)$$

Here r_p is the classical proton radius. The second form of Eq. (10) is obtained by introducing the normalized emittance $\varepsilon = 4\pi\gamma\sigma^2/\beta$, which is an invariant during acceleration in a proton synchrotron, in the absence of beam blow-up. Therefore, the beam-beam strength parameter for head-on collisions is also independent of energy. Note that the normalized emittance is defined with a numerical factor 6π at Fermilab. Of course, Eqs. (1) and (2) remain valid for protons and may be used when $\sigma_x \neq \sigma_y$ and/or $\beta_x \neq \beta_y$.

3.1 Recent observations

In this section I shall summarize recent observations in the SPS at CERN [25] and the Tevatron [26] at Fermilab. Table 2 shows the relevant parameters and observations of beam-beam strength parameters in the two machines. It calls for a series of comments:

(i) There are 12 head-on beam-beam collisions around the Tevatron, but only 3 head-on collisions in the SPS because the beams are horizontally separated over most of its circumference.

(ii) In both machines, the bunchlength is not small compared to β, hence the luminosity is 2/3 of the figure which can be calculated from Eq. (10) and the data in Table 2.

(iii) In both machines the proton bunches are more intense and have a larger emittance than the antiproton bunches, such that the beam-beam strength parameters ξ^+ and ξ^- differ by less than a factor 3/2 which brings both machines into the strong-strong configuration.

	SPS		Tevatron	
	p	$\bar{p}$	p	$\bar{p}$
Energy E/GeV	315		900	
Part./bunch $N/10^{10}$	11	5	7	2.5
Bunches/beam k	6	6	6	6
Norm.emittance ε μm	12π	7π	16π	8π
Bunch area A/eVs	0.7	0.5	3.0	3.0
BB strength $\xi_x/10^{-3}$	4.9	5.2	1.5	2.1
BB strength $\xi_y/10^{-3}$	3.5	3.7	1.5	2.1
Luminosity $L/cm^{-2}s^{-1}$	1.8×10^{30}		1.7×10^{30}	

Table 2 - Parameters of proton colliders

3.2 Interpretation

3.2.1 Tune spreads. The observations in the SPS and the Tevatron agree that the tunes must be kept between two resonant values, and this must be done for all particles in the beam including any tune spread which they may have. Both machines operate in the neighbourhood of the coupling resonance $\{Q_x\}=\{Q_y\}$ where $\{..\}$ denotes the fractional part. The particular regions selected are shown in Table 3, together with their width and the lowest order resonance inside the region. There are two main sources for tune spread:

Machine	Tune range	Width	Resonance
SPS	2/3 - 7/10	0.0333	11/16
Tevatron	2/5 - 3/7	0.0286	5/12

Table 3 - SPS and Tevatron operating regions

(i) The beam-beam effect causes a tune spread of the order of ξ for each head-on collision, and a smaller value for each separated collision. In the Tevatron, all collisions are head-on and the total tune spread ΔQ is approximately $\Delta Q \approx 12\xi$. Accurate calculations, taking into account the amplitude functions and dispersions at the collision points yield slightly

smaller values. The tune spread is independent of energy. Comparing the tune spread to the space between resonances leads to the beam-beam limit $\xi < 0.0024$, quite close to the observed values shown in Table 2. Indeed, it is found in the Tevatron that the beam emittance ε must be larger than a minimum value and/or the bunch intensity N must be smaller than a maximum value, such that their ratio N/ε, which is proportional to ξ, stays below an upper limit. In the SPS, the bunches collide in three, and are well separated in the remaining nine collision points. Hence, the total tune spread $\Delta Q = 3\xi$. Comparing this to the space between resonances leads to the beam-beam limit $\xi \approx 0.01$, while the actual observed value shown in Table 2 is about half as much.

(ii) A second source of tune spread is the direct space-charge effect (Laslett tune shift) which causes particles with large synchrotron oscillation amplitudes to experience the full tune shift when they are at the centre of the bunch and hardly any tune shift at all when they are at the head or tail of the bunch. In the SPS, this effect causes a tune spread $\Delta Q_{SC} \approx 0.035$ at the injection energy, 26 GeV. It is comparable to the space between resonances and therefore believed to present an upper limit on the bunch population [25]. A closer look reveals that the direct space-charge effect in the approximation of round beams, neglecting the contribution of the momentum spread to the beam size, is proportional to the ratio N/ε, called the beam brightness at Fermilab, as is the beam-beam strength parameter ξ. Since for given N/ε the direct space-charge effect scales like γ^{-2} it is unimportant in the Tevatron with injection at 150 GeV.

3.2.2 Density distributions and lifetime. Observations at the Tevatron [26] show that the density distributions of both proton and antiprotons are very well approximated by a Gaussian at injection. Once the beams are accelerated and the amplitude functions β squeezed to a low value, the density distribution of the protons remains a Gaussian, while the distribution of the antiprotons is higher in the core, narrower in the flanks, and higher in the tails than a Gaussian with the same area and standard deviation.

Observations at the SPS [25] show a clear dependence on the ratio of the proton and antiproton emittance. In 1987, the proton emittance was about four times the antiproton emittance. This not only reduced the proton lifetime at the beginning of the coast to less than 10 hours, but also created intolerably high background rates for the physics experiments. In 1988, the proton emittance was about a factor of two smaller than in 1987, and the emittance ratio less than two. Within minutes after the start of a coast, the proton lifetime increased to about 50 hours and the background became tolerable. It should be remembered that the luminosity lifetime in the SPS is limited by intra-beam scattering [28].

For the SPS, this behaviour is explained by the presence of high order nonlinear resonances within the tune spread (5/12 in the Tevatron, 11/16 in the SPS). Their widths increase with the amplitude of the test particle, and the maximum width moves to higher amplitudes as the order increases [27]. When the emittance of the test beam is larger than the emittance of the driving beam, more test particles reach dangerous amplitudes than in the case of similar emittances.

3.3 Conclusions for proton colliders

Both proton colliders, SPS and Tevatron, operate with more intense and larger proton than antiproton beams, such that the beam-beam strength parameters acting on protons and antiprotons, ξ^+ and ξ^-, are almost balanced for the SPS, while for the Tevatron $\xi^- \approx 3/2\ \xi^+$. Both machines exploit the tune space between resonances of moderate order: the SPS for accommodating the direct space-charge tune spread at injection, the Tevatron for accommodating the total tune spread due to twelve beam-beam collisions. Therefore, the Tevatron is limited by the beam-beam effect while the SPS is not. The SPS observes that the narrower antiproton beam causes losses from the tails of the wider proton beam and a lifetime reduction, while the opposite is observed in the Tevatron.

4. Final remarks

Beam-beam effects in electron and proton colliders are a field of active research. Much has been learned from observations. In electron colliders the beam-beam limit stabilized around $\xi_y = 0.03$, while in proton colliders it is determined by the tune space available between resonances of moderate order. Novel theoretical techniques for studying the beam-beam effect in electron colliders have been tried on simplified models. They hold the promise of eventually explaining the beam-beam limit if the difficulties associated with more realistic models can be overcome.

Acknowledgements

The author gratefully acknowledges helpful correspondance and discussions with D. Finley, J. Gareyte, K. Hirata and R. Schmidt.

References

1. G.E. Fischer, SPEAR-154 (1972).
2. Spear Group, IEEE Trans Nucl.Sci. NS-20 (1973) 838.
3. K. Satoh et al., Proc. 6th Symp. Accel. Sci. Technology (Tokyo) 18.
4. N.N., Status of Beijing collider, this conference.
5. E. Keil and R. Talman, Part. Acc. 14 (1983) 109.
6. A. Piwinski, Proc. 8th Int. Conf. High Energy Accel. CERN (1971) 357.
7. A. Chao and E. Keil, CERN/ISR-TH/79-31 (1979).
8. R. Talman, AIP Conf. Proc. 153 (1987) 789.
9. E. Keil, Nucl. Instr. Meth. 188 (1981) 9.
10. E. Keil, CERN LEP Note 294 (1981).
11. K. Hirata, Nucl. Instr. Meth. A269 (1988) 7.
12. A. Hofmann and S. Myers, CERN LEP Note 604 (1988).
13. R.E. Meller and R.H. Siemann, IEEE Trans. Nucl. Sci. NS-28 (1981) 2431.
14. K. Yokoya, TRISTAN Design Note, TN-890001 (1989).
15. A. Piwinski, Proc. 11th Int. Conf. High Energy Accel., Geneva 1980 (Birkhäuser, 1980) 751.
16. S. Peggs and R. Talman, ibid. 754.
17. S. Myers, IEEE Trans. Nucl. Sci. NS-28 (1981) 2503.
18. S. Myers, Nucl. Instr. Meth. 211 (1983) 263.
19. K. Hirata, Phys. Rev. D37 (1988) 1307.
20. M.A. Furman, K.Y. Ng and A.W. Chao, SSC-174 (1988).
21. M.H.R. Donald and J.M. Paterson, IEEE Trans. Nucl. Sci. NS-26 (1979) 3580.
22. K. Hirata, these proceedings.
23. Y.H. Chin, these proceedings.
24. Y.H. Chin, LBL-25370 (1988).
25. L. Evans, J. Gareyte, M. Meddahi and R. Schmidt, these proceedings.
26. G. Dugan, these proceedings.
27. L.R. Evans, CERN 84-15 (1984) 319.
28. L.R. Evans, Proc. 12th Int. Conf. High Energy Accel. (1983) 229.